BULLETIN OF THE POLISH ACADEMY OF SCIENCES
TECHNICAL SCIENCES, Vol. 63, No. 3, 2015
DOI: 10.1515/bpasts-2015-0088

A problem of optimal cylindricity profile matching

D. JANECKI*, J. ZWIERZCHOWSKI, and L. CEDRO

Faculty of Mechatronics and Mechanical Engineering, Kielce University of Technology, 7 Al. Tysiąclecia P.P. St., 25-314 Kielce, Poland

Abstract. The bird-cage strategy used for measuring cylindricity is reported to be the most effective, as it provides the most detailed information about an analyzed object. The average values of profiles measured with the cross-section and the generatrix strategies may differ slightly, yet this may result from some design imperfections of the measurement instruments used. In this study, the problem of optimal profile matching is formulated and solved. As a result, the differences between the values of the registered profiles at the points of intersection of the scanning trajectories can be minimized.

Key words: cylindricity, bird-cage strategy, profile matching.

1. Introduction

Rotary components constitute a large and important group of machine parts. They are common, for instance, in the automotive, power, paper and shipbuilding industries; therefore, one of the most significant metrological tasks today is to ensure maximum accuracy of roundness and cylindricity measurements [1–7].

Cylindrically shaped objects have generally been assessed by measuring their roundness deviations at several cross-sections. In practice however, the reliability of a product is dependent on the whole area of the surface. It is desirable that cylindrical components be evaluated by means of the parameters that refer to the whole surface area.

Cylindricity needs to be measured in such a way that the representation of the measured surface is as precise as possible. It is important to ensure appropriate density of measuring points. The basic criterion for selecting a measurement strategy is to assume the predominant harmonic for both roundness and straightness profiles. In practice, it is difficult to cover the entire surface with measuring points using the theoretical minimum density of points defined in the ISO 12180 standard [8]. The standard describes the measurement strategies that provide specific rather than general information about cylindrically shaped objects. These are: the cross-section strategy, the generatrix strategy, the bird-cage strategy being a combination of the previous two, and the point strategy (see Fig. 1).

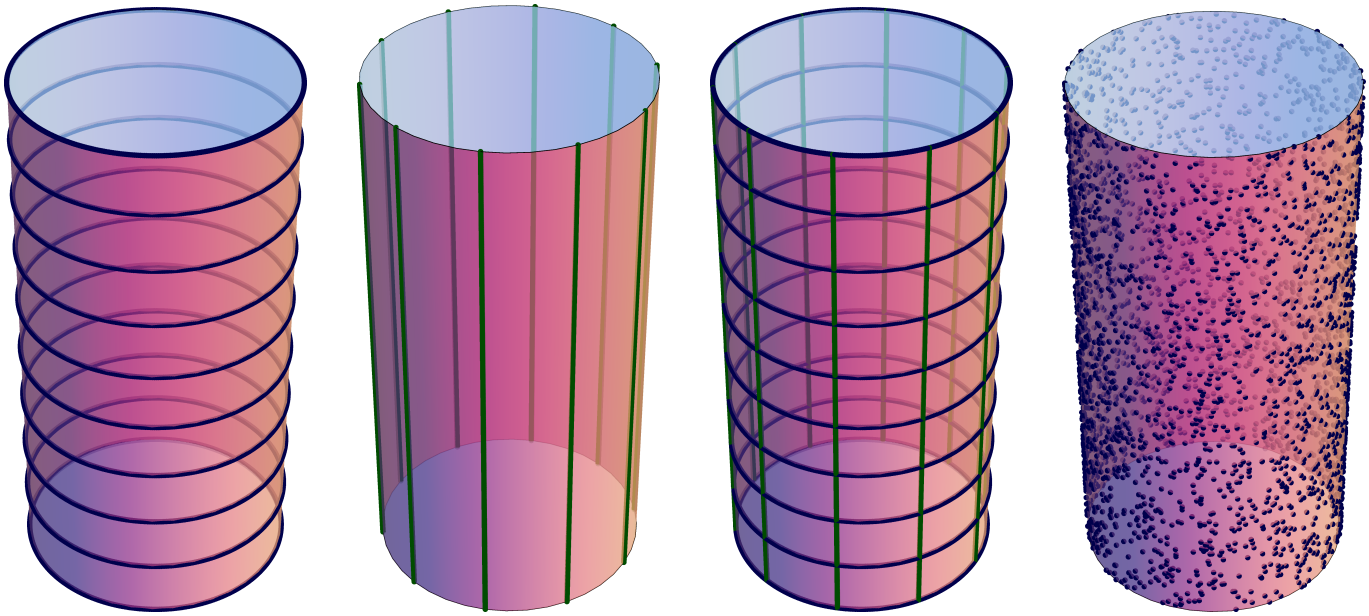

Fig. 1. Cylindricity measurement strategies, according to the ISO 12180 standard (left to right): the cross-section strategy, the generatrix strategy, the bird-cage strategy, the points strategy

*e-mail: djanecki@tu.kielce.pl

The cross-section and the generatrix strategies are implemented in the majority of instruments applying the radial method. The point strategy is frequently employed when form deviations are assessed by means of coordinate measuring machines. The ISO 12180 standard recommends using the bird-cage strategy. Surprisingly, it is not commonly used to measure cylindricity deviations even though it provides the most detailed information about measured objects [9].

It appears that the average values of profiles measured with the cross-section and the generatrix strategies differ slightly. This may be due to certain design imperfections of the measurement instruments used. In this study, the problem of optimal profile matching is formulated and solved. As a consequence, the differences between the values of the registered profiles at the points of intersection of the scanning trajectories can be minimized.

2. The bird-cage cylindricity measurement strategy

Let us consider an XYZ Cartesian coordinate system associated with the measurement table of the instrument where the Z-axis coincides with the spindle rotation axis. It is also convenient to apply a cylindrical coordinate system because the radial method of measurement of the macrogeometry of cylindrical surfaces involves scanning the object surface during the spindle rotation and the vertical shift of the sensor. The coordinates of a point in the cylindrical system associated with the XYZ system are represented by three numbers (φ, r, z), where φ is the angular coordinate of the point, r is the radial coordinate (distance of the point from the Z-axis), and z is the height-related coordinate. A cylindrical surface can be written parametrically using a function:

$$r_{\mathrm{cyl}}(\varphi, z), \qquad 0 \le \varphi \le 2\pi, \qquad 0 \le z \le H. \tag{1}$$

The bird-cage strategy applied to measure the cylindricity of rotary objects combines the principles of the cross-section and the generatrix strategies. It is assumed that the instrument is equipped with high precision systems for measuring the sensor height and the angle of table or spindle rotation.

When a profile is to be measured at a selected cross-section, the vertical shift of the sensor is switched off. The sensor needs to be shifted to a desired height and the table or spindle rotation switched on. The moment the control system receives a signal of the zero angular position, the measurement starts. It is assumed that the height coordinates of the consecutive cross-sections are:

$$z_n, \qquad n = 1, 2, ..., N, \tag{2}$$

where N denotes the number of cross-sections. Then, without loss of generality, we assume that the height coordinates of the consecutive sections are arranged in ascending order and

$$0 = z_1 < z_2 < ... < z_N = H. \tag{3}$$

In order to simplify the notation and to avoid troublesome indexing over samples of the profile we assume that the measured profiles are continuous functions of the variables z and φ. Thus the values of the profile observed in the subsequent cross-sections are denoted by $r_n^c(\varphi)$. Obviously, measurements performed with the radial method are relative in character, thus

$$r_n^c(\varphi) \cong \rho + r_{\mathrm{cyl}}(\varphi, z_n), \qquad n = 1, 2, ..., N \tag{4}$$

for an unknown value of ρ. The approximation symbol $\cong$ emphasize that the measurements of the profile radius contain errors resulting from the measurement noise and the instrument design imperfections. If the coordinates z_n of the cross-sections are uniformly distributed over the range $[0, H]$, then $z_n = H \cdot (n-1)/(N-1)$, $n = 1, 2, ..., N$.

Profile measurements at longitudinal sections are performed with the table (spindle) at standstill. A measurement commences after the table is turned to a desired angular position and the vertical sensor shift is switched on. The sensor position can be stabilized by applying an additional run-up section several millimeters in length. Therefore, it is essential that the height of the sensor after switching on the shift be smaller than the initial height of the analyzed cylindricity profile. Assume that the angular coordinates of the longitudinal sections are:

$$\varphi_m, \qquad m = 1, 2, ..., M, \tag{5}$$

where M denotes the number of sections. The values of the profile at the consecutive longitudinal sections are denoted by:

$$r_m^g(z) \cong \rho + r_{\mathrm{cyl}}(\varphi_m, z), \qquad m = 1, 2, ..., M. \tag{6}$$

Additionally, if we assume that the angular coordinates φ_m of the longitudinal sections are uniformly distributed in the range $[0, 2\pi]$, then $\varphi_m = 2\pi(m-1)/M$, $m = 1, 2, ..., M$.

The points of intersection of the scanning trajectories will play an important role in this study. These coordinates are (φ_m, z_n), $m = 1, ..., M$, $n = 1, ..., N$, while the values of the profile radius are $r_n^c(\varphi_m)$ and $r_m^g(z_n)$ respectively.

3. The problem of optimal profile matching

When a cylindricity measurement conducted by means of the bird-cage strategy is completed, one can observe that the values of the profile radius at the points of intersection of the scanning trajectories in the cross and longitudinal sections are slightly different. The difference may be due to some imperfections of the sensor system design. Note that the measurement conditions for the cross-section strategy are different from those for the generatrix strategy. This causes different distribution of forces acting on the sensor tip. Imperfections of the hydrostatic bearing used in the table spindle are another possibility. The position of the table may differ if measurements are performed with the table in a rotary motion (cross-sections) or with the table at stand still (longitudinal sections). As a result, the profile observed with the cross-section strategy can be slightly shifted in relation to the profile observed with the generatrix strategy.

3.1. Comparing the measurement results obtained by the cross-section and the generatrix strategies.

A profile shift can be best observed in a spatial diagram of measuring points

in a cylindrical coordinate system (φ, z, r). Figure 2 illustrates the results of a series of cylindricity measurements performed on a radial cylindricity measurement instrument. The points obtained by means of the cross-section and the generatrix strategies are drawn in dark and light gray, respectively (blue and green when printed in color). The first three measurements were conducted for rollers with a diameter of 52 mm and a height of 100 mm, each. The surface preparation involved polishing (the first two specimens) or grounding (the third specimen). Note that there is a clear difference in the waviness level between the polished and the grounded cylinders. The last three measurements were carried out for rollers with a diameter of 38 mm and a height of 62 mm, each. Such rollers are used in bearings. In all the cases considered, the measurements were taken in the central part of the cylindrical workpieces 10 mm away from the bases.

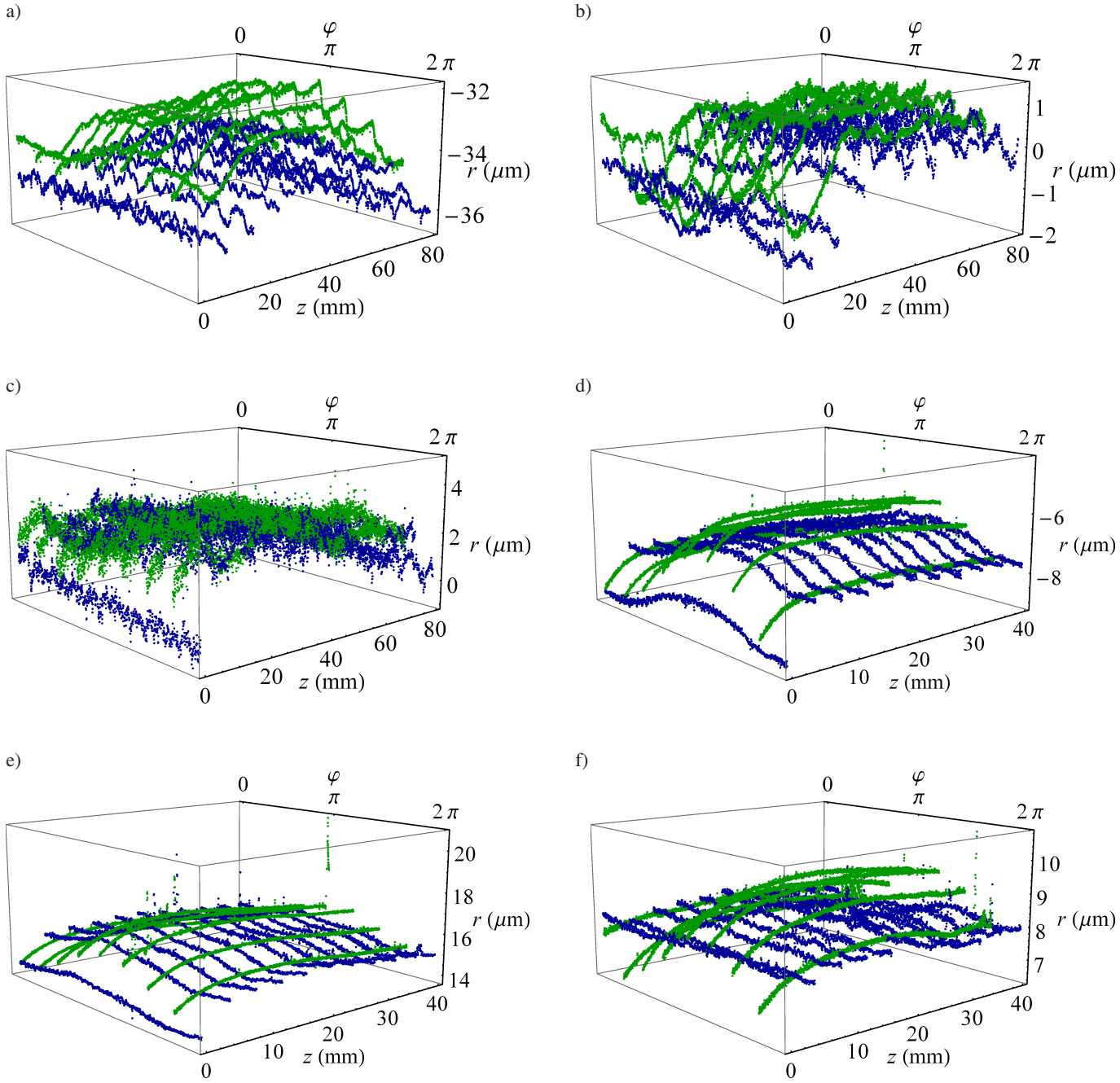

Fig. 2. Examples of 3D plots of the measuring points in the cylindrical coordinate system

As can be seen, there is a clear positive shift in value of straightness profiles in relation to roundness ones. The calculations were performed separately for the cross-section strategy and the generatrix strategy. The values are presented in Table 1. As can be seen, the differences in the mean profile radius range from 0.2 to more than 1.0 μm.

Table 1
Average values of the profiles obtained by means of the cross-section R_o^c and the generatrix R_o^g strategies – comparison of cross and longitudinal sections

Sample	R_o^c [μm] cross sections	R_o^g [μm] longitudinal sections	Difference $R_o^g - R_o^c$ [μm]
a	−34.7	−33.3	1.38
b	−0.166	0.279	0.446
c	1.74	2.05	0.309
d	−7.22	−6.92	0.300
e	15.4	15.9	0.417
f	8.04	8.43	0.391

3.2. Formulation and solution of the problem of optimal profile matching. Let us first consider an ideal measuring instrument with error-free representation of the cylindricity profile $r_{\mathrm{cyl}}(\varphi, z)$. If apply the bird-cage strategy, we obtain then the following set of values of the profile radius:

$$r_n^c(\varphi) = \rho + r_{\mathrm{cyl}}(\varphi, z_n), \qquad n = 1, 2, ..., N, \tag{7}$$

$$r_m^g(z) = \rho + r_{\mathrm{cyl}}(\varphi_m, z), \qquad m = 1, 2, ..., M, \tag{8}$$

for an unknown value of ρ. In this case, at the points of intersection of profile scanning paths, the condition

$$r_n^c(\varphi_m) = r_m^g(z_n) \tag{9}$$

is fulfilled. Due to measurement errors, the above condition is fulfilled only approximately. At the first step, we could assume that due to the instrument imperfections, the difference between the observed radii $r_n^c(\varphi_m) - r_m^g(z_n)$ at points (φ_m, z_n) is constant. Let us consider, however, a more general case. Assume that the difference between the actual and the observed profiles is different for each cross-section. Thus,

$$r_n^c(\varphi) \cong \rho_n^c + r_{\mathrm{cyl}}(\varphi, z_n), \qquad n = 1, 2, ..., N, \tag{10}$$

$$r_m^g(z) \cong \rho_m^g + r_{\mathrm{cyl}}(\varphi_m, z), \qquad m = 1, 2, ..., M \tag{11}$$

for unknown values of ρ_m^c and ρ_n^g. Now, it is essential to calculate the values of ρ_m^c and ρ_n^g so that the difference $r_n^c(\varphi_m) - r_m^g(z_n)$ is the smallest possible. Taking into account the above relationships, we obtain:

$$\begin{gathered} r_n^c(\varphi) - \rho_n^c \cong r_m^g(z_n) - \rho_m^g, \\ n = 1, 2, ..., N, \qquad m = 1, 2, ..., M. \end{gathered} \tag{12}$$

The number of equations $N \cdot M$ is much bigger than the number of unknown parameters. Furthermore, it should be noted that each measurement signal contains a noise. It is thus reasonable to introduce an appropriate index of profile matching. Let us define the corrected profiles

$$\widehat{r}_n^c(\varphi) = r_n^c(\varphi) - \rho_n^c, \qquad n = 1, 2, ..., N, \tag{13}$$

$$\widehat{r}_m^g(z) = r_m^g(z) - \rho_m^g, \qquad m = 1, 2, ..., M \tag{14}$$

and the quadratic profile matching error

$$\begin{aligned} &J(\rho_1^c, ..., \rho_N^c, \rho_1^g, ..., \rho_M^g) \\ &= \frac{1}{2} \sum_{n=1}^{N} \sum_{m=1}^{M} \left(\widehat{r}_n^c(\varphi_m) - \widehat{r}_m^g(z_n) \right)^2. \end{aligned} \tag{15}$$

The values of $\rho_1^c, ..., \rho_N^c, \rho_1^g, ..., \rho_M^g$ minimizing the index J are calculated by equating the partial derivatives $\partial J / \partial \rho_n^c$ and $\partial J / \partial \rho_m^g$ to zero. Thus, we obtain a system of equations that can be written in the matrix form

$$\mathbf{A}\boldsymbol{\rho} = \mathbf{b}, \tag{16}$$

where

$$\boldsymbol{\rho} = [\ \rho_1^c \quad \dots \quad \rho_N^c \quad \rho_1^g \quad \dots \quad \rho_M^g\ ]^T, \tag{17}$$

$$\mathbf{A} = \begin{bmatrix} M & & & -1 & \cdots & -1 \\ & \ddots & & \vdots & \ddots & \vdots \\ & & M & -1 & \cdots & -1 \\ -1 & \cdots & -1 & N & & \\ \vdots & \ddots & \vdots & & \ddots & \\ -1 & \cdots & -1 & & & N \end{bmatrix} \begin{matrix} \left.\vphantom{\begin{matrix} a \\ a \\ a \end{matrix}}\right\} N \\ \left.\vphantom{\begin{matrix} a \\ a \\ a \end{matrix}}\right\} M \end{matrix},$$

$$\mathbf{b} = \begin{bmatrix} \sum_{m=1}^{M} (r_1^c(\varphi_m) - r_m^g(z_1)) \\ \vdots \\ \sum_{m=1}^{M} (r_N^c(\varphi_m) - r_m^g(z_N)) \\ -\sum_{n=1}^{N} (r_n^c(\varphi_1) - r_1^g(z_n)) \\ \vdots \\ -\sum_{n=1}^{N} (r_n^c(\varphi_M) - r_M^g(z_n)) \end{bmatrix}. \tag{18}$$

It is easy to check that this system of Eqs. (16) has infinitely many solutions. Indeed, if ρ_n^c and ρ_m^g constitute a certain solution to the system of equations, then the values of $\rho_n^c + \varepsilon$ and $\rho_m^g + \varepsilon$ for a certain value of ε are also a solution to this system. Without loss of generality, we can reject the first equation from the system (16) and assume that the signal shift for the first roundness profile ρ_1^c is equal to zero. Alternatively, the minimization problem (15) can be supplemented with one additional equality constraint. For example, we can demand that the average value of all profiles after profile matching be equal to zero, that is

$$\frac{1}{2\pi N} \sum_{n=1}^{N} \int_0^{2\pi} \widehat{r}_n^c(\varphi) \mathrm{d}\varphi + \frac{1}{HM} \sum_{m=1}^{M} \int_0^{H} \widehat{r}_m^g(z) \mathrm{d}z = 0. \tag{19}$$

In this way, we obtain an additional equation:

$$\frac{1}{N}\sum_{n=1}^{N}\rho_n^c+\frac{1}{M}\sum_{m=1}^{M}\rho_m^g = \frac{1}{2\pi N}\sum_{n=1}^{N}\int_0^{2\pi} r_n^c(\varphi)\mathrm{d}\varphi+\frac{1}{HM}\sum_{m=1}^{M}\int_0^{H} r_m^g(z)\mathrm{d}z. \tag{20}$$

After calculating the values of the parameters ρ_n^c and ρ_m^g, we modify the value of the observed profile in accordance with the formulae (13) and (14).

4. The generalized problem of optimal profile matching

The approach presented in the previous section can be generalized. The axis of rotation in the instruments with a rotary table may be dependent to a certain degree on the rotational velocity of the table.. The position of the axis of rotation may differ if measurements are performed by means of the cross-section strategy (with the table in rotary motion) and the generatrix strategy (with the table at standstill). The change in the position of the table rotation axis can be compensated for by modifying the measured profiles according to the following relationship:

$$\widehat{r}_n^c(\varphi)=r_n^c(\varphi)-\rho_n^c,\quad n=1,...,N, \tag{21}$$

$$\widehat{r}_m^g(z)=r_m^g(z)-\rho_m^g-(c_x^g+d_x^g z)\cos\varphi_m -(c_y^g+d_y^g z)\sin\varphi_m, \quad m=1,2,...,M, \tag{22}$$

where c_x^g, d_x^g, c_y^g, d_y^g are additional parameters defining the reciprocal position of the table axes. Note that the relative eccentricity c_x^g and c_y^g can be compensated for by selecting freely the parameters ρ_m^g. We can, therefore, assume that $c_x^g=c_y^g=0$. Finally, the parameters responsible for the profile matching are calculated by minimizing the index (15), which is now dependent on the parameters $\rho_1^c,...,\rho_N^c$, $\rho_1^g,...,\rho_M^g$, d_x^g, d_y^g. From the necessary conditions for optimality we obtain

$$\begin{bmatrix}\mathbf{A} & \mathbf{L}^T\\ \mathbf{L} & \mathbf{K}\end{bmatrix}\begin{bmatrix}\boldsymbol{\rho}\\ \mathbf{d}\end{bmatrix}=\begin{bmatrix}\mathbf{b}\\ \mathbf{e}\end{bmatrix}, \tag{23}$$

where

$$\mathbf{L}^T=\begin{bmatrix} -z_1\sum_{m=1}^{M}\cos\varphi_m & -z_1\sum_{m=1}^{M}\sin\varphi_m\\ \vdots & \vdots\\ -z_N\sum_{m=1}^{M}\cos\varphi_m & -z_N\sum_{m=1}^{M}\sin\varphi_m\\ \cos\varphi_1\sum_{n=1}^{N}z_n & \sin\varphi_1\sum_{n=1}^{N}z_n\\ \vdots & \vdots\\ \cos\varphi_M\sum_{n=1}^{N}z_n & \sin\varphi_M\sum_{n=1}^{N}z_n\end{bmatrix}, \tag{24}$$

$$\mathbf{K}=\left(\sum_{n=1}^{N}z_n^2\right)\cdot\begin{bmatrix}\sum_{m=1}^{M}\cos^2\varphi_m & \sum_{m=1}^{M}\cos\varphi_m\sin\varphi_m\\ \sum_{m=1}^{M}\cos\varphi_m\sin\varphi_m & \sum_{m=1}^{M}\sin^2\varphi_m\end{bmatrix}, \tag{25}$$

$$\mathbf{d}=\begin{bmatrix} d_x^g & d_y^g\end{bmatrix}^T \tag{26}$$

and

$$\mathbf{e}=\begin{bmatrix}\sum_{n=1}^{N}\sum_{m=1}^{M}z_n\sin\varphi_m\left(r_n^c(\varphi_m)-r_m^g(z_n)\right)^2\\ \sum_{n=1}^{N}\sum_{m=1}^{M}z_n\sin\varphi_m\left(r_n^c(\varphi_m)-r_m^g(z_n)\right)^2\end{bmatrix}. \tag{27}$$

Like in the previous case, we can assume that $\rho_1^c=0$ and then reject the first equation in the system (23). However, we can apply a different approach. In the algorithm described above, measurements of the profiles of the cylinder generatrices can be properly modified so that the axis of the mean cylinder of these profiles will coincide with the axis of the mean cylinder of the profiles measured in the cross-sections. It is also possible to introduce additional parameters; as a result, after profile matching, we immediately obtain profiles for which the mean axis coincides with the Z-axis and the average value of the profile is equal to zero. Thus, after profile matching, we immediately obtain a deviation of the profiles from the mean cylinder. Now let us assume that the corrected profiles are described with the following equations

$$\widehat{r}_n^c(\varphi)=r_n^c(\varphi)-\rho_n^c-(c_x^c+d_x^c z_n)\cos\varphi -(c_y^c+d_y^c z_n)\sin\varphi, \quad n=1,...,N, \tag{28}$$

$$\widehat{r}_m^g(z)=r_m^g(z)-\rho_m^g-d_x^g z\cos\varphi_m-d_y^g z\sin\varphi_m, \quad m=1,2,...,M. \tag{29}$$

Like in the previous case, we assume that $c_x^g=c_y^g=0$. Now, the profile matching index is dependent on the parameters $\rho_1^c,...,\rho_N^c$, c_x^c, c_y^c, d_x^c, d_y^c, $\rho_1^g,...,\rho_M^g$, d_x^g, d_y^g, among which there are five free parameters ρ_1^c, c_x^c, c_y^c, d_x^c, d_y^c. To solve the index minimization problem, we introduce five additional equality conditions. Let us define the parameters of the mean cylinder of all the observed profiles ρ^a, c_x^a, d_x^a, c_y^a, d_y^a, where the parameter ρ^a defines the radius of the mean cylinder, while the other parameters refer to the cylinder axis coordinates.

The term '*mean cylinder*' is clearly defined for the whole surface area of the cylinder (1). It is assumed that the parameters of this cylinder minimize the index

$$J^a(\rho_n^a,c_x^a,d_x^a,c_y^a,d_y^a) = \frac{1}{2\pi H}\int_0^{2\pi}\int_0^{H}\left(r_{\mathrm{cyl}}(\varphi,z)-\rho_n^a-(c_x^a+d_x^a z)\cos\varphi -(c_y^a+d_y^a z)\sin\varphi\right)^2\mathrm{d}\varphi\mathrm{d}z. \tag{30}$$

We assume the following equivalent of the definition of the mean cylinder for the bird-cage strategy

$$\begin{aligned} & J^a(\rho^a, c_x^a, d_x^a, c_y^a, d_y^a) \\ &= \frac{1}{2\pi N} \sum_{n=1}^{N} \int_0^{2\pi} (\widehat{r}_n^c(\varphi) - \rho^a - (c_x^a + d_x^a z_n)\cos\varphi \\ &\quad -(c_y^a + d_y^a z_n)\sin\varphi)\,\mathrm{d}\varphi \\ &+ \frac{1}{HM} \sum_{m=1}^{M} \int_0^{H} (\widehat{r}_m^g(z) - \rho^a - (c_x^a + d_x^a z)\cos\varphi_m \\ &\quad -(c_y^a + d_y^a z)\sin\varphi_m)\,\mathrm{d}z. \end{aligned} \tag{31}$$

We obtain the additional five equality constraints by calculating the partial derivatives of the index (31) with respect the mean cylinder parameters; we compare these derivatives to zero and finally assume that

$$\rho^a = c_x^a = d_x^a = c_y^a = d_y^a = 0. \tag{32}$$

The calculation details are omitted here.

5. Experiments

The effects of the application of the profile matching algorithms will be analyzed basing on the measurements of two rollers with a diameter of 52 mm and a height of 100 mm, each. One specimen was polished and the other was ground. The measurements were conducted for the following parameters of the bird-cage strategy:

$$N = 11; \qquad M = 8. \tag{33}$$

The cross and longitudinal sections are distributed uniformly over the ranges of angle and height changeability, $[0, 2\pi]$ and $[0, H]$, respectively. Two measures of profile matching quality are considered: the root-mean-square and the arithmetic mean of the difference in the radii at the points of intersection of the cross and longitudinal section paths

$$\Delta r_{nm} \stackrel{\mathrm{df}}{=} r_m^g(z_n) - r_n^c(\varphi_m), \tag{34}$$

i.e.

$$\Delta R_{\mathrm{QM}} \stackrel{\mathrm{df}}{=} \sqrt{\frac{1}{NM} \sum_{n=1}^{N} \sum_{m=1}^{M} (\Delta r_{nm})^2}, \tag{35}$$

$$\Delta R_{\mathrm{AM}} \stackrel{\mathrm{df}}{=} \frac{1}{NM} \sum_{n=1}^{N} \sum_{m=1}^{M} \Delta r_{nm}. \tag{36}$$

Hereafter, the expression Δr_{nm} will be called the *difference in the radii at the points of intersection* or briefly *difference in the radii*.

5.1. The roller with polished surface. Figure 3a shows a plot of measuring points in the cylindrical coordinate system. As can be seen, there is a clear positive shift of profiles at the longitudinal sections in relation to those at the cross-sections. The difference is more visible in the bar plot of difference in the radii at the points of intersection in Fig. 3b. The root-mean-square and the arithmetic mean of the difference in the radii before matching were:

$$\Delta R_{\mathrm{QM}} = 0.632\ \mu\mathrm{m}, \quad \Delta R_{\mathrm{AM}} = 0.465\ \mu\mathrm{m}$$

respectively. As we can see, the profile shift reaches almost half a μm. After the application of the profile matching algorithm described in previous Section the root-mean-square and the arithmetic mean of the difference in the radii were:

$$\Delta R_{\mathrm{QM}} = 0.109\ \mu\mathrm{m}, \quad \Delta R_{\mathrm{AM}} = 0$$

respectively.

The results of the optimal matching algorithm are very satisfactory. The root-mean-square of the difference in the radii decreased approximately sixfold. The zero value of the arithmetic mean is obvious and results from the least squares principle. The next figures show plots of the profile and difference in the radii after matching.

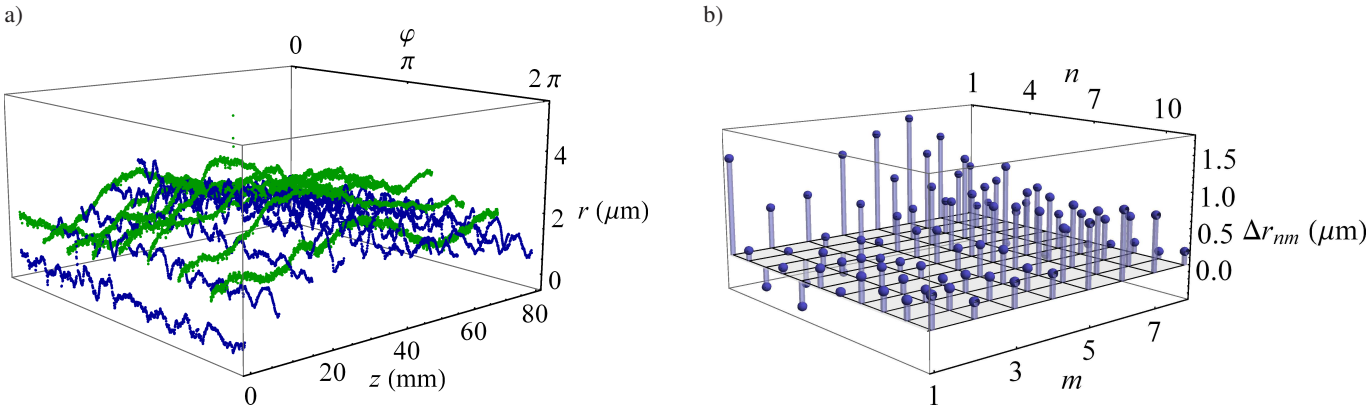

Fig. 3. a) 3D plot of the measuring points in the cylindrical coordinate system b) a bar plot of difference in the radii at the points of intersection: surface after polishing

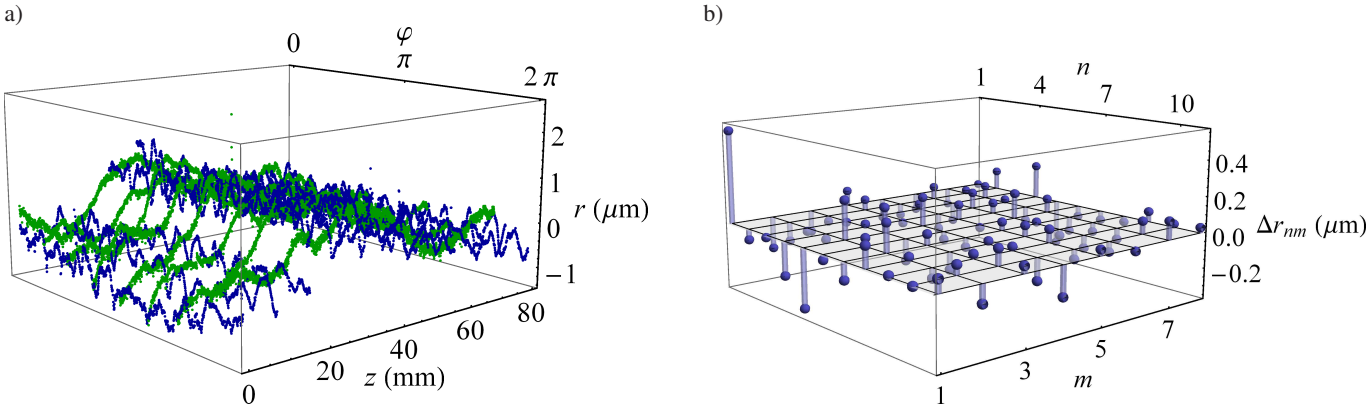

Fig. 4. The measuring points and the difference in the radii after profile matching: surface after polishing

5.2. The roller with ground surface. The tests were repeated for the roller with ground surface, see Fig. 5, 6. The root-mean-square and the arithmetic mean of the difference in the radii before matching were:

$$\Delta R_{\mathrm{QM}} = 0.480\ \mu\mathrm{m}, \quad \Delta R_{\mathrm{AM}} = 0.277\ \mu\mathrm{m}$$

respectively. The profile shift is considerably smaller than that in the previous case. This testifies to large randomness of the shift phenomenon. The root-mean-square of the difference in the radii after profile matching is

$$\Delta R_{\mathrm{QM}} = 0.235\ \mu\mathrm{m}.$$

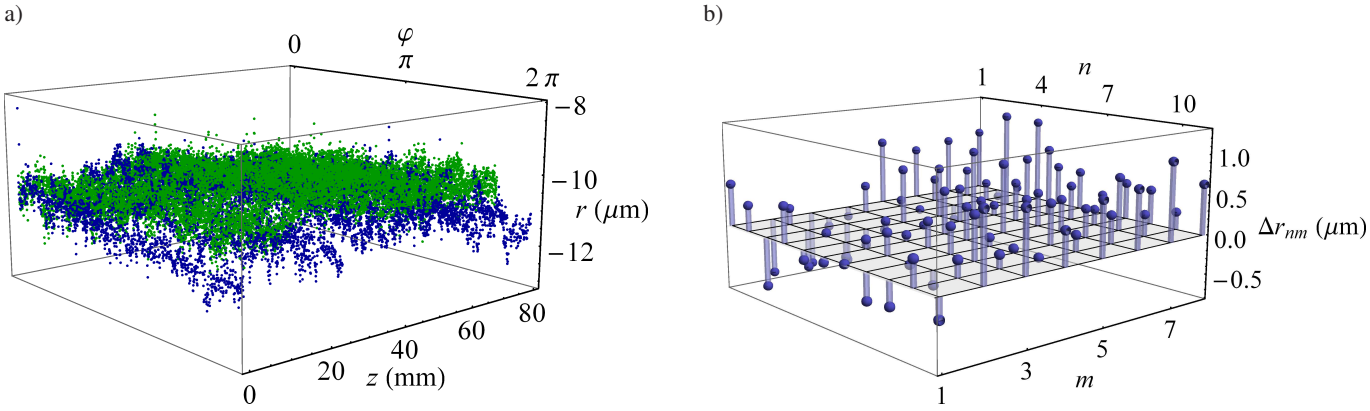

Fig. 5. The measuring points and the difference in the radii: surface after grinding

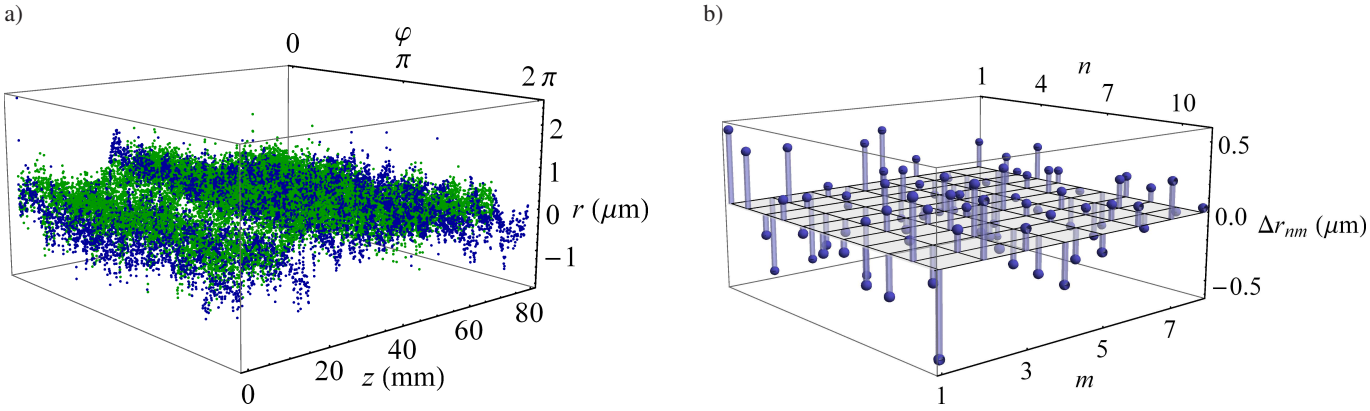

Fig. 6. The measuring points and the difference in the radii after profile matching: surface after grinding

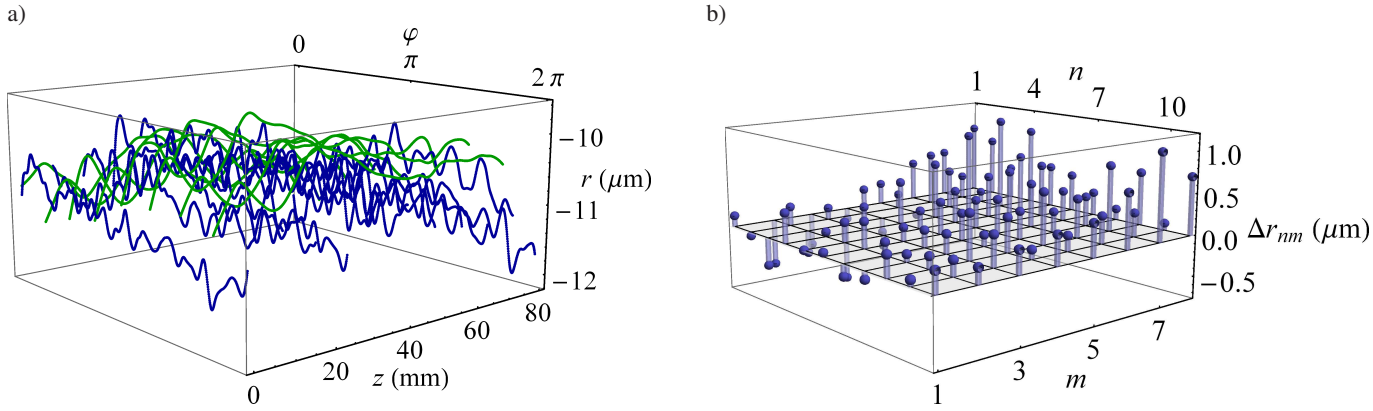

Fig. 7. The measuring points and the difference in the radii after profile filtering: surface after grinding

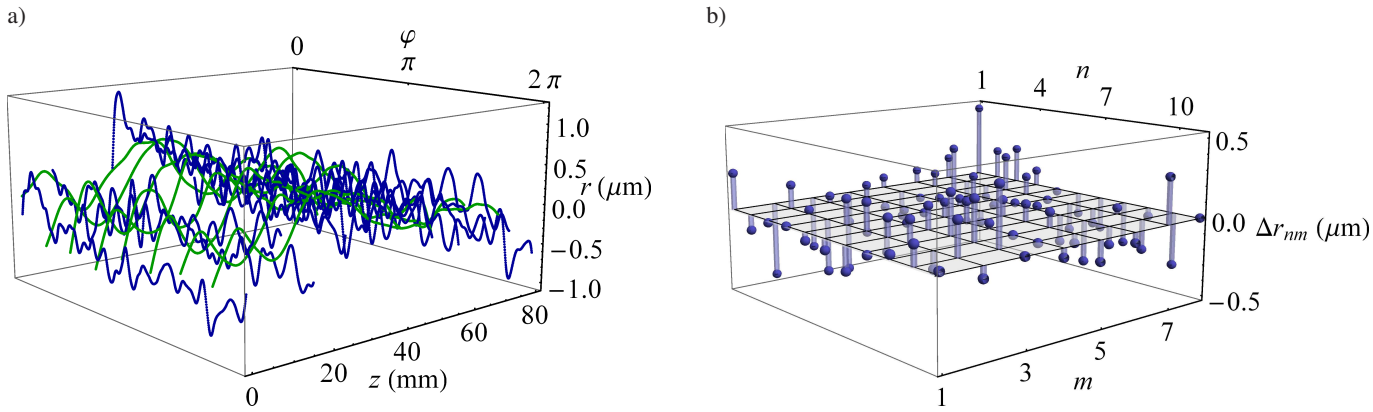

Fig. 8. The measuring points and the difference in the radii after profile filtering and matching: surface after grinding

As can be seen, the average difference in the radii decreases only twofold. This is due to the occurrence of a large profile waviness component. The influence of the waviness on the value of the profile for given coordinates (φ, z) is rather accidental, as was shown in Ref. [10]. The influence of the waviness is more significant when the number of cross-sections in the bird-cage strategy is smaller. It seems justifiable that in the case of occurrence of a strong waviness component on the measured surface, the measured profiles are filtered using an appropriate low-pass filter, which rejects waviness components. In the case considered here, a spline filter [11, 12] with cutoff wavelength $\lambda_c = 8$ mm was used. After profile filtration, the mean values of the difference in the radii are

$$\Delta R_{\mathrm{QM}} = 0.442\ \mu\mathrm{m}, \quad \Delta R_{\mathrm{AM}} = 0.301\ \mu\mathrm{m}$$

and, as we can see, these values are close to those calculated for the primary profiles. After applying the profile matching algorithm, the value of the root-mean-square is

$$\Delta R_{\mathrm{QM}} = 0.154\ \mu\mathrm{m}.$$

As can be seen, now the value of the profile matching error decreases threefold. Figures 7 and 8 show diagrams of filtered profiles and a diagram of difference in the radii before and after profile matching.

6. Conclusions

The results of the measurements conducted by means of the bird-cage strategy for various cylindrically shaped objects show a shift in the average values of the profile measured with the cross-section and the generatrix strategies. The shift may be up to tenths of the micrometer, and, in extreme cases, more than a micrometer. The shift is probably due to a different distribution of forces acting on the sensor tip during measurements with the cross-section and the generatrix strategies. To eliminate the errors, it was necessary to formulate and solve the problem of optimal profile matching, which involved shifting the profile values at the consecutive cross-sections in such a way that the difference in the radii at the points of intersection of the scanning trajectories was the smallest possible. The results of the experiment show that due to the optimal profile matching, the root-mean-square of the difference in the radii at the points of intersection of the scanning trajectories may decrease from several to several dozen times depending on the level of the waviness component.

References

[1] S.-Y. Chou and C.-W. Sun, "Assessing cylindricity for oblique cylindrical features", *Int. J. Machine Tools & Manufacture* 40 (3), 327–341 (2000).

[2] K.D. Summerhays, R.P. Henke, J.M. Balwin, R.M. Casssou, and C.W. Brown, "Optimizing discrete point sample patterns and measurement data analysis on cylindrical surfaces with systematic form deviations", *Precision Engineering* 26 (1), 105–121 (2002).

[3] W. Gao, J. Yokoyama, H. Kojima, and S. Kiyono, "Precision measurement of cylinder straightness using a scanning multi-probe system", *Precision Engineering* 26 (3), 279–288 (2002).

[4] Y.-Z. Lao, H.-W. Leong, F.P. Preparata, and G. Singh, "Accurate cylindricity evaluation with axis-estimation preprocessing", *Precision Engineering* 27 (4), 429–437 (2003).

[5] K. Stępień nad W. Makieła, "An analysis of deviations of cylindrical surfaces with the use of wavelet transform", *Metrology and Measurement Systems* 20 (1), 139–150 (2013).

[6] D.G. Chetwynd, "A unified approach to the measurement analysis of nominally circular and cylindrical surfaces", *Doctoral Thesis*, University of Leicester, Leicester, 1980.

[7] S. Adamczak, D. Janecki, W. Makieła, and K. Stępień, "Quantitative comparison of cylindricity profiles measured with different methods using Legendre-Fourier coefficients", *Metrology and Measurement Systems* 17 (3), 397–404 (2010).

[8] ISO/TS 12180: Geometrical Product Specifications (GPS) – Cylindricity – Part 1: Vocabulary and parameters of cylindrical form, Part 2: Specification operators, 2003.

[9] S. Adamczak, D. Janecki, and J. Świderski, "Combined roundness and straightness measurement applied to the assessment of cylindricity profiles of machine parts", *Measurement Automation and Monitoring* 54 (5), 248–250 (2008).

[10] S. Adamczak, D. Janecki, and R. Domagalski, "Experimental significance of the calculation of harmonic components in roundness and waviness profiles", *Measurement Automation and Monitoring* 46 (5), 17–20 (2000).

[11] M. Krystek, "Form filtering by splines", *Measurement* 18 (1), 9–15 (1996).

[12] D. Janecki, "A two-dimensional isotropic spline filter", *Precision Engineering* 37 (4), 948–965 (2013).